Available online at www.sciencedirect.com
ScienceDirect
Trans. Nonferrous Met. Soc. China 23(2013) 2644−2649
Transactions of Nonferrous Metals Society of China
www.tnmsc.cn

Sulfurization synthesis and photocatalytic activity of oxysulfide $La_3NbS_2O_5$

Xin-de TANG[1], Hong-qi YE[2], Han-xiang HU[1]

1. Department of Materials and Chemical Engineering, Hunan Institute of Technology, Hengyang 421002, China;
2. School of Chemistry and Chemical Engineering, Central South University, Changsha 410083, China

Received 9 July 2012; accepted 26 November 2012

Abstract: The oxysulfide $La_3NbS_2O_5$ was synthesized by sulfurization using H_2S and characterized by X-ray diffraction (XRD), UV−Vis diffuse reflectance spectroscopy (DRS) and field emission scanning electron microscopy (FE-SEM). The relationship between the sulfurization conditions and the photocatalytic activities for H_2 evolution was investigated. Sulfurization method allowed for synthesis of $La_3NbS_2O_5$ at much lower temperatures and significantly shortened reaction time of 1 h compared with conventional solid-state techniques. The particle morphologies were regular platelike with sizes of 0.1−0.6 μm and smooth surfaces. The highest activity for H_2 evolution was obtained at 1073 K for 1 h, which was about 1.83 times that of $La_3NbS_2O_5$ prepared by solid-state method.

Key words: sulfurization method; H_2 evolution; $La_3NbS_2O_5$; photocatalysis; visible light

1 Introduction

Since the discovery of photoelectric splitting of water on TiO_2 electrodes by FUJISHIMA and HONDA in 1972 [1], the photocatalytic water splitting using solar energy and semiconductors to generate clean energy hydrogen has attracted increasing attention [2−7]. A large number of photocatalysts consisting of metal ions with d^0 and d^{10} electron configurations have been developed for photocatalytic H_2 and O_2 evolution from water to date [8−12]. However, these photocatalysts are not active under visible light. Therefore, the development of photocatalysts with visible-light response would be valuable for application to H_2 production using solar energy. Metal oxysulfides are candidates for visible-light responsive photocatalysts, and promising results have been reported for $Sm_2Ti_2S_2O_5$ [13,14], La_3GaS_5O [15], $La_2O_2S_2$ [16], $ZnS_{1-x-0.5y}O_x(OH)_y$ [17]. Recently, oxysulfide $La_3NbS_2O_5$ with large particle size has been synthesized by a solid-state reaction method [18], and its photocatalytic activity is very low [19]. Solid-state synthetic procedures provide relatively limited or no control over particle sizes or morphologies. By contrast, sulfurization synthetic methods have shown the ability to accelerate the relatively slow diffusion of reactants and to control the crystal growth of metal oxysulfides particles [20]. Further, it have been demonstrated that surface morphology as well as particle size are significant factors in photocatalytic activity [21], and the use of fine particles with good crystallinity is favorable for photocatalysis [22]. Thus, sulfurization synthetic methods are appropriate for probing the effects of particle morphologies and sizes on their photocatalytic activities, and which will lead to new insights on the origins of their photocatalytic activities.

In this work, the sulfurization synthesis of oxysulfide $La_3NbS_2O_5$ was investigated. Measurements of their photocatalytic activities for H_2 evolution were performed in a 0.01 mol/L Na_2S−Na_2SO_3 solution, and the relationship between the sulfurization conditions and the photocatalytic activities for H_2 evolution was investigated, along with a comparison of the photocatalytic activity of the new material with that of the products obtained from the solid-state methods.

2 Experimental

2.1 Synthesis of $La_3NbS_2O_5$

Powder samples of La_3NbO_7 were prepared by a polymerized complex (PC) method using $NbCl_5$ and $La(NO_3)_3·6H_2O$ as starting materials [23]. Methanol was

Foundation item: Projects (11JJ3020, 10JJ9015) supported by Hunan Provincial Natural Science Foundation of China; Project supported by the Construct Program of the Key Discipline in Hunan Province, China
Corresponding author: Xin-de TANG; Tel: +86-734-3452163; E-mail: txd759@sina.com
DOI: 10.1016/S1003-6326(13)62780-6

employed as solvents, and anhydrous citric acid and ethylene glycol were employed as a complexing agent to immobilize Nb and La ions. After polymerization of a mixture containing stoichiometric amounts of La and Nb (La/Nb=3:1) according to the method in Ref. [24], La_3NbO_7 was obtained by calcination at 773 K in air. This La_3NbO_7 is referred to as the oxide precursor. The oxide precursors (0.5 g) were placed in quartz carrier and then were placed in tubular furnace. Powder samples of $La_3NbS_2O_5$ were prepared from the oxide precursors by calcination under flowing H_2S (flow rate of 10 mL/min) at various temperatures for various time. The solid-state preparation of $La_3NbS_2O_5$ followed the reported procedures [18].

2.2 Characterization of catalysts

The crystal structure of prepared samples was analyzed by the powder X-ray diffraction (D/Max 2500 VB+, Japan) with Cu K_α radiation (λ=0.154056 nm).The particle microstructures and approximate sizes of prepared samples were determined by FE-SEM (Sirion 200, Philips, Netherlands).

Surface area of prepared samples was measured on a surface area analyzer (Autosorbi/monosorb, Quantachrme, America) by N_2 absorption at 77 K using the Brunauer Emmett Teller (BET) method. The DRS of prepared samples was obtained using a UV–Vis scanning spectrophotometer (TU-1901, Beijing-Purkinje, China) at room temperature, and was converted from reflectance to absorbance by the Kubelka–Munk method.

2.3 Photocatalytic testing

Reactions were carried out in an inner-irradiation quartz reaction vessel connected to a glass closed gas circulation system. The powder catalyst (1 g) was dispersed and suspended in a 0.01 mol/L Na_2S−Na_2SO_3 solution (570 mL) under magnetic stirring. The cocatalyst Pt (1.0%, mass fraction) was loaded by impregnation from H_2PtCl_6 followed by reduction in H_2 at 473 K for 2 h. The reactant solution was evacuated several times to remove air completely prior to irradiation using a 250 W high-pressure Xe arc lamp. For visible irradiation (λ> 400 nm), a sodium nitrite ($NaNO_2$) aqueous solution (2 mol/L) was inserted in the light path used to block ultraviolet (UV) light. The gases evolved in the reaction were analyzed by gas chromatography (Shimadsu GC-8A, Japan, Ar carrier). The number of photons reaching the solution was measured with a Si photodiode. The apparent quantum efficiencies were calculated using the equation: $Q=(AR/I)\times100\%$, where A, R, and I are coefficients based on the reactions (H_2 evolution, 2), the H_2 evolution rate (molecules h^{-1}), and the rate of absorption of incident photons (7.2×10^{21} photons h^{-1} at 400 nm≤λ≤600 nm based on the total photon number reaching the reaction solution).

3 Results and discussion

Figure 1 shows the XRD patterns of $La_3NbS_2O_5$ prepared by sulfurization method at 1123 K for different sulfurization time. For comparison, Fig. 1 also shows the XRD patterns of $La_3NbS_2O_5$ prepared at 1273 K for 9 d by the solid-state method. Diffraction peaks corresponding to $La_3NbS_2O_5$ appeared for the sample sulfurized after 0.5 h. After 1 h sulfurization, the diffraction peaks of La_3NbO_7 disappeared. At sulfurization time for 1 or 2 h, a single phase of $La_3NbS_2O_5$ was obtained. Thus, the sulfurization method allows for very quick synthesis of $La_3NbS_2O_5$ compared with the solid-state method, which took up to 9 d. Figure 2 shows the XRD patterns of $La_3NbS_2O_5$ obtained at various sulfurization temperatures for 1 h. The power XRD analysis showed that $La_3NbS_2O_5$ calcined at 1073 K or above was a single phase. In the case of the samples

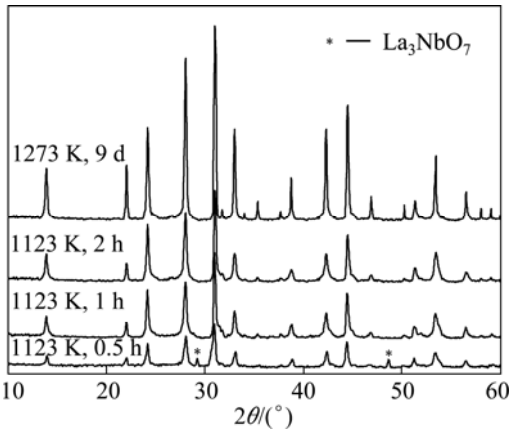

Fig. 1 XRD patterns of $La_3NbS_2O_5$ prepared at 1123 K for different sulfurization time and at 1273 K for 9d by a solid-state method

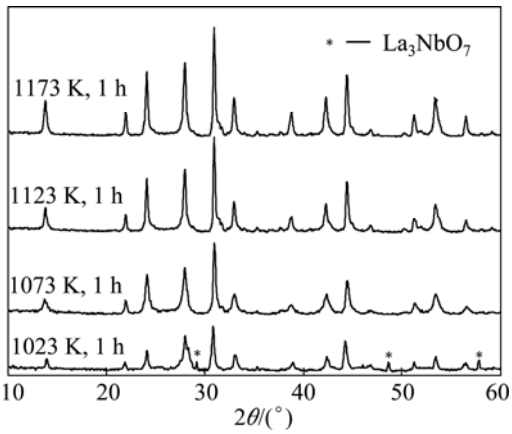

Fig. 2 XRD patterns of $La_3NbS_2O_5$ obtained at various sulfurization temperatures

calcined at 1023 K, most of the peaks in XRD patterns were attributed to $La_3NbS_2O_5$, but relatively weak peaks due to La_3NbO_7 were also observed. With increasing temperature from 1023 to 1173 K, the major peaks became narrower and their intensity increased.

Table 1 lists the crystallite size and BET area of $La_3NbS_2O_5$ sulfurization samples with sulfurization temperature and time. The crystallite sizes of $La_3NbS_2O_5$ samples were determined by the Scherrer equation, using the (105) reflection of $La_3NbS_2O_5$ for calculation. The BET area of $La_3NbS_2O_5$ samples was measured on a surface area analyzer by N_2 absorption at 77 K using the BET method. With sulfurization temperature from 1023 to 1173 K, the crystallite size of $La_3NbS_2O_5$ increased gradually, and the BET area of $La_3NbS_2O_5$ decreased gradually. The crystallite size of $La_3NbS_2O_5$ prepared at 1123 K for 0.5 h was estimated to be about 57.3 nm, and continued to grow with sulfurization time. The BET area of $La_3NbS_2O_5$ prepared at 1123 K for 0.5 h was estimated to be about 6.67 m^2/g, and continued to decrease with sulfurization times. For comparison, Table 1 also shows the crystallite size and BET area of the solid-state preparation of $La_3NbS_2O_5$ samples. Because of calcination at high temperatures over a long period, the crystallite size of $La_3NbS_2O_5$ prepared by solid-state method was larger than that of $La_3NbS_2O_5$ prepared by sulfurization method, while the BET area of $La_3NbS_2O_5$ prepared by solid-state method was significantly less than that of $La_3NbS_2O_5$ prepared by sulfurization method.

Table 1 Crystallite size and BET area of $La_3NbS_2O_5$ samples

Catalyst sample (LNSO(T-h)[(a)])	Crystallite size/nm	BET area/($m^2 \cdot g^{-1}$)
LNSO(1023-1)	51.5	9.32
LNSO(1073-1)	55.2	7.04
LNSO(1123-0.5)	57.3	6.67
LNSO(1123-1)	58.8	6.35
LNSO(1123-2)	60.5	6.02
LNSO(1173-1)	62.6	5.81
LNSO(SSR)[b]	92.7	0.65

(a) $La_3NbS_2O_5$ sample calcined at a certain temperature for a certain sulfurization time, e.g. LNSO(1023-1) denotes $La_3NbS_2O_5$ sample calcined at 1023 K for 1 h; (b) $La_3NbS_2O_5$ sample prepared by solid-state method

Figure 3 shows SEM images of $La_3NbS_2O_5$ prepared by the solid-state and sulfurization methods. In the case of $La_3NbS_2O_5$ prepared by the solid-state methods, irregular block-like particles with sizes of 1−3 μm as well as a lot of smaller size particles were observed. In the case of $La_3NbS_2O_5$ prepared by the

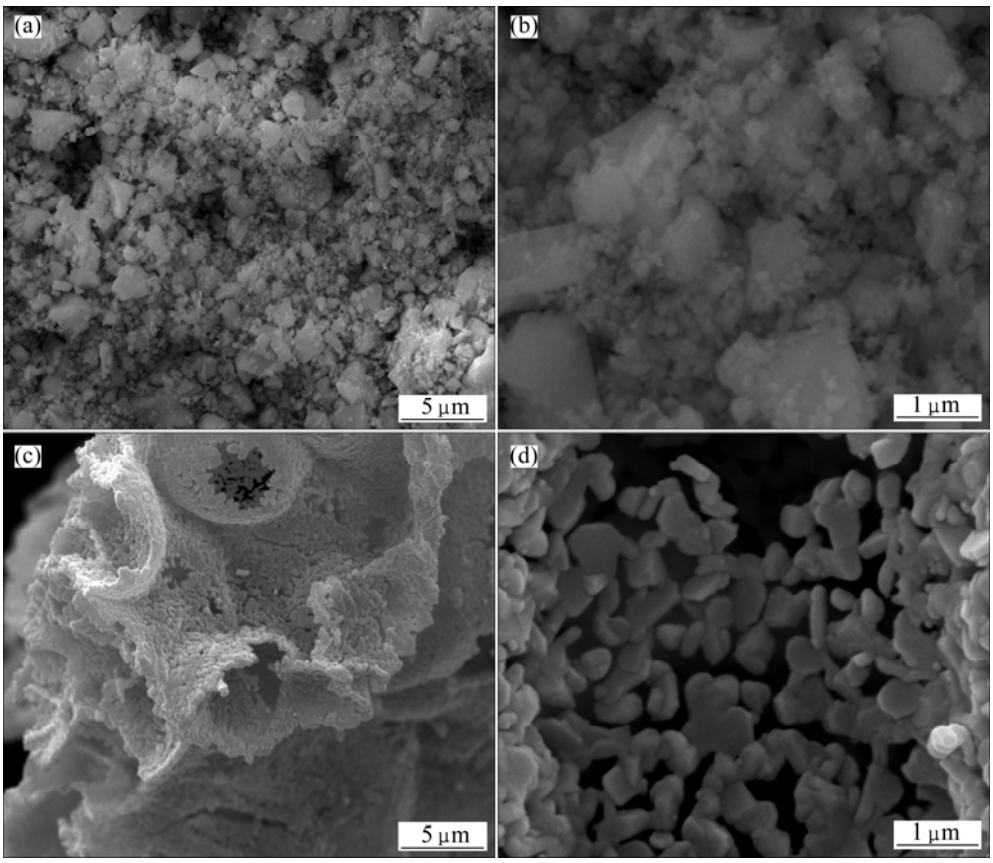

Fig. 3 SEM images of $La_3NbS_2O_5$ prepared by solid-state (a, b) and sulfurization (c, d) methods

sulfurization methods, platelike particles with smooth surfaces were obtained, and their particle sizes were 0.1−0.6 μm. The difference in the particle size between those calculated by the Scherrer equation and those observed by SEM suggests that the particles observed by SEM are the polycrystalline particles. It was found that the morphology of $La_3NbS_2O_5$ prepared by sulfurization methods was relatively constant, and independent of sulfurization temperature. This similar phenomenon had also been reported for $Sm_2Ti_2S_2O_5$ [14].

The optical properties of photocatalytic materials were very important because they dictated the number of photons absorbed by the system. Figure 4 shows the DRS of $La_3NbS_2O_5$ prepared under varying sulfurization conditions and a solid-state procedure. It was found that all of $La_3NbS_2O_5$ showed obvious absorption in the visible light range (>400 nm) irrespective of the preparation conditions. The optical absorptions of $La_3NbS_2O_5$ prepared by sulfurization method were slightly attenuated with increasing sulfurization time and temperature, and were obviously higher than that of $La_3NbS_2O_5$ prepared by the solid-state method. Using the formula E_g/eV=1240/λ_g, where λ_g (nm) was extrapolated from the linear rise in the absorption curve, the band gaps of the sulfurization synthesized $La_3NbS_2O_5$ were calculated to be in the range of 2.13−2.17 eV, and the band gap of the solid-state synthesized $La_3NbS_2O_5$ was calculated to be about 2.26 eV.

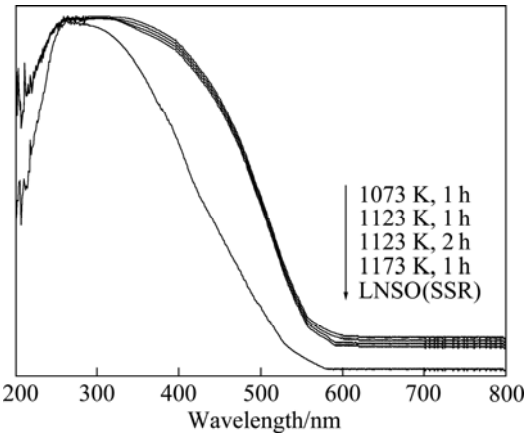

Fig. 4 DRS of $La_3NbS_2O_5$ prepared under varying sulfurization conditions and solid-state procedure

In order to test the effects of the sulfurization synthesis conditions on its photocatalytic activity, each sample was tested for photocatalytic H_2 evolution in an inner-irradiation quartz reaction vessel in a 0.01 mol/L Na_2S−Na_2SO_3 solution. Table 2 shows the rate of H_2 evolution of $La_3NbS_2O_5$ prepared under varying sulfurization conditions and a solid-state procedure. The highest activity of H_2 evolution (11×10^{-6} mol/h) was obtained for the sample prepared at 1073 K for 1 h by sulfurization method, which was about 1.83 times that obtained by the solid-state method due to larger surface area (see Table 1) and higher optical absorption (see Fig. 4). The quantum efficiency for H_2 evolution was about 0.092% for the $La_3NbS_2O_5$ sample prepared at 1073 K for 1 h. In contrast, the quantum efficiencies of H_2 evolutions for $La_3NbS_2O_5$ (SSR) were estimated to be about 0.05%. The photocatalytic activity of $La_3NbS_2O_5$ prepared at 1023 K for 0.5 h was lower than that of the sample prepared at 1123 K for 0.5 h due to lower crystallinity (see Table 1), and the photocatalytic activity of $La_3NbS_2O_5$ prepared at 1023 K for 1 h was lower than that of the sample prepared at 1073K for 1 h due to lower crystallinity and impurity La_3NbO_7. Also, the photocatalytic activity of $La_3NbS_2O_5$ prepared at 1123 K for 0.5 h was lower than that of the sample prepared at 1123 K for 1 h due to lower crystallinity and impurity La_3NbO_7, and the photocatalytic activity of $La_3NbS_2O_5$ prepared at 1123 K for 2 h was lower than that of the sample prepared at 1123 K for 1 h due to particle growth. The photocatalytic activity decreased with increasing sulfurization temperature from 1073 to 1173 K. Because crystal structures of $La_3NbS_2O_5$ prepared by different sulfurization temperatures were uniform, and morphology of $La_3NbS_2O_5$ prepared by different sulfurization temperatures was relatively constant. Particle growth and slightly attenuated optical absorptions with increasing sulfurization temperature were considered to be responsible for the reduced photocatalytic activities. Thus, it was all-important to control the sulfurization conditions which had an important influence on photocatalytic activity of oxysulfide $La_3NbS_2O_5$.

Table 2 Rate of H_2 evolution of $La_3NbS_2O_5$ prepared under varying sulfurization conditions and solid-state procedure

Catalyst sample	Rate of H_2 evolution/(10^{-6} mol·h^{-1})
LNSO(1023-1)	3
LNSO(1073-1)	11
LNSO(1123-0.5)	7
LNSO(1123-1)	10
LNSO(1123-2)	8
LNSO(1173-1)	5
LNSO(SSR)	6

4 Conclusions

1) The oxysulfide $La_3NbS_2O_5$ was synthesized by sulfurization method at much lower temperatures and

significantly shortened reaction times of 1.0 h compared to conventional solid-state techniques.

2) With increasing sulfurization temperature and time, the crystallite size of $La_3NbS_2O_5$ increased gradually, and the BET area of $La_3NbS_2O_5$ decreased gradually. The optical band gaps of sulfurization synthetic $La_3NbS_2O_5$ were 2.13−2.17 eV, which were less than that (2.26 eV) of $La_3NbS_2O_5$ prepared by conventional solid-state techniques.

3) Photocatalytic activities of sulfurization synthetic $La_3NbS_2O_5$ in a 0.01 mol/L Na_2S−Na_2SO_3 solution were 3×10^{-6}−11×10^{-6} mol/h, and the maximum rate was about 1.83 times that of $La_3NbS_2O_5$ prepared by solid-state method.

References

[1] FUJISHIMA A, HONDA K. Electrochemical photolysis of water at a semiconductor electrode [J]. Nature, 1972, 238(53−58): 37−38.

[2] ZOU Z, YE J, SAYAMA K, ARAKAWA H. Direct splitting of water under visible light irradiation with an oxide semiconductor photocatalyst [J]. Nature, 2001, 414(6864): 625−627.

[3] ASAHI R, MORIKAWA T, OHWAKI T, AOKI K, TAGA Y. Visible-light photocatalysis in nitrogen-doped titanium oxides [J]. Science, 2001, 293 (5528): 269−271.

[4] MAEDA K, TERAMURA K, LU D, TAKATA T, SAITO N, INOUE Y, DOMEN K. Photocatalyst releasing hydrogen from water-Enhancing catalytic performance holds promise for hydrogen production by water splitting in sunlight [J]. Nature, 2006, 440(7082): 295−295.

[5] WANG X, MAEDA K, THOMAS A, TAKANABE K, XIN G, CARLSSON J M, DOMEN K, ANTONIETTI M. A metal-free polymeric photocatalyst for hydrogen production from water under visible light [J]. Nature Mater, 2009, 8: 76−80.

[6] CHEN X, LIU L, YU P Y, MAO S S. Increasing solar absorption for photocatalysis with black hydrogenated titanium dioxide nanocrystals [J]. Science, 2011, 331: 746−752.

[7] ZHANG J, YU J, ZHANG Y, LI Q, GONG J R. Visible-light photocatalytic h_2-production activity of CuS/ZnS porous nanosheets based on photoinduced interfacial charge transfer[J]. Nano Lett, 2011, 11(11): 4774−4779.

[8] KATO H, ASAKURA K, KUDO A. Highly efficient water splitting into H_2 and O_2 over lanthanum-doped $NaTaO_3$ photocatalysts with high crystallinity and surface nanostructure [J]. J Am Chem Soc, 2003, 125 (10): 3082−3089.

[9] OGURA S, SATO K, INOUE Y. Effects of RuO_2 dispersion on photocatalytic activity for water decomposition of $BaTi_4O_9$ with a pentagonal prism tunnel and $K_2Ti_4O_9$ with a zigzag layer structure [J]. Phys Chem Chem Phys, 2000, 2(10): 2449−2454.

[10] MISEKI Y, KATO H, KUDO A. Water splitting into H_2 and O_2 over $Cs_2Nb_4O_{11}$ photocatalyst [J]. Chem Lett, 2005, 34(1): 54−55.

[11] SATO J, SAITO S, NISHIYAMA H, INOUE Y. Photocatalytic water decomposition by RuO_2-loaded antimonates, $M_2Sb_2O_7$ (M=Ca, Sr), $CaSb_2O_6$ and $NaSbO_3$, with d^{10} configuration [J]. J Photochem Photobiol A, 2002, 148(1−3): 85−89.

[12] SATO J, KOBAYASHI H, KARASHI K, SAITO N, NISHIYAMA H, INOUE Y. Photocatalytic activity for water decomposition of RuO_2-dispersed Zn_2GeO_4 with d(10) configuration [J]. J Phys Chem B, 2004, 108(14): 4369−4375.

[13] ISHIKAWA A, TAKATA T, KONDO J, HARA M, KOBAYASHI H, DOMEN K. Oxysulfide $Sm_2Ti_2S_2O_5$ as a stable photocatalyst for water oxidation and reduction under visible light irradiation ($\lambda\leq650$ nm) [J]. J Am Chem Soc, 2002, 124(45): 13547−13553.

[14] ISHIKAWA A, YAMADA Y, TAKATA T, KONDO J, HARA M, KOBAYASHI H, DOMEN K. Novel synthesis and photocatalytic activity of oxysulfide $Sm_2Ti_2S_2O_5$ [J]. Chem Mater, 2003, 15(23), 4442−4446.

[15] OGISU K, ISHIKAWA A, SHIMODAIRA Y, TAKATA T, KOBAYASHI H, DOMEN K. Electronic band structures and photochemical properties of La−Ga-based oxysulfides [J]. J Phys Chem C, 2008, 112(31): 11978−11984.

[16] OHASHI M, ISHIGAKI T, UEMATSU K, TODA K, SATO M. Low temperature synthesis method of $La_2O_2S_2$ and evaluation of the photocatalytic activity [J]. Key Eng Mater, 2010, 445: 217−220.

[17] LI Yue-xiang, MA Gang-feng, PENG Shao-qin, LU Gong-xuan, LI Shu-ben. Photocatalytic H_2 evolution over basic zincoxysulfide ($ZnS_{1-x-0.5y}O_x(OH)_y$) under visible light irradiation [J]. Appl Catal A, 2009, 363(1−2): 180−187.

[18] CARIO L, POPA A, LAFOND A, GUILLOT-DEUDON C, KABBOUR H, MEERSCHAUT A, CLARKE S, ADAMSON P. Cation deficient layered ruddlesden-popper-related oxysulfides $La_2LnMS_2O_5$ (Ln=La, Y; M=Nb, Ta) [J]. Inorg Chem, 2007, 46: 9584−9590.

[19] OGISU K. Some (Oxy) sulfide materials as visible light driven photocatalysts for water splitting reaction [D]. Tokyo: Department of Chemical System Engineering, School of Engineering, The University of Tokyo, 2009: 88−90.

[20] ISHIKAWA A, TAKATA T, MATSUMURA T, KONDO J N, HARA M, KOBAYASHI H, DOMEN K. Oxysulfides $Ln_2Ti_2S_2O_5$ as stable photocatalysts for water oxidation and reduction under visible-light irradiation [J]. J Phys Chem B, 2004, 108(8): 2637−2642.

[21] POROB D, MAGGARD P J. Flux syntheses of La-doped $NaTaO_3$ and its photocatalytic activity [J]. J Solid State Chem, 2006, 179: 1727−1732.

[22] YAO Mao-hai, TANG You-gen, ZHANG Li, YANG Hai-hua, YAN Jian-hui. Photocatalytic activity of CuO towards HER in catalyst from oxalic acid solution under simulated sunlight irradiation [J]. Transactions of Nonferrous Metals Society of China, 2010, 20: 1944−1949.

[23] MILANOVA M M, KAKIHANA M, ARIMA M, YASHIMA M, YOSHIMURA M. A simple solution route to the synthesis of pure $La_2Ti_2O_7$ and $Nd_2Ti_2O_7$ at 700−800 °C by polymerized complex method [J]. J Alloys Compd, 1996, 242(1−2): 6−10.

[24] ABE R, HIGASHI M, SAYAMA K, ABE Y, SUGIHARA H. Photocatalytic Activity of R_3MO_7 and $R_2Ti_2O_7$ (R=Y, Gd, La; M =Nb, Ta) for Water Splitting into H_2 and O_2 [J]. J Phys Chem B, 2006, 110: 2219−2226.

硫氧化物 $La_3NbS_2O_5$ 的硫化合成及其光催化活性

唐新德[1]，叶红齐[2]，胡汉祥[1]

1. 湖南工学院 材料与化学工程学院，衡阳 421002；
2. 中南大学 化学化工学院，长沙 410083

摘　要：采用 H_2S 硫化的方法合成硫氧化物 $La_3NbS_2O_5$，并通过 X 射线衍射(XRD)、紫外−可见漫反射(DRS)、场发射扫描电镜(FE-SEM)等技术对其进行表征和分析，研究硫化条件与光催化分解水产氢活性的关系。结果表明：与传统固相法比较，硫化法使 $La_3NbS_2O_5$ 在更低的温度和更短的反应时间(1 h)合成；合成的 $La_3NbS_2O_5$ 粒子呈规则的盘子状，粒径为 0.1−0.6 μm，粒子表面光滑；在 1073 K 硫化 1 h 制得的 $La_3NbS_2O_5$ 具有极高的产氢活性，大约为固相法制得 $La_3NbS_2O_5$ 的产氢活性的 1.83 倍。

关键词：硫化法；产氢；$La_3NbS_2O_5$；光催化；可见光

(Edited by Chao WANG)